



HAL
open science

An innovative device for in vivo and in vitro study of fragrance evaporation after application on skin or model surfaces

Elise Hadjiefstathiou, Daria Terescenco, Vincent Loisel, Céline Picard,
Catherine Malhiac, Géraldine Savary

► To cite this version:

Elise Hadjiefstathiou, Daria Terescenco, Vincent Loisel, Céline Picard, Catherine Malhiac, et al.. An innovative device for in vivo and in vitro study of fragrance evaporation after application on skin or model surfaces. *Talanta*, 2024, 281, 10.1016/j.talanta.2024.126851 . hal-04695520

HAL Id: hal-04695520

<https://hal.science/hal-04695520>

Submitted on 12 Sep 2024

HAL is a multi-disciplinary open access archive for the deposit and dissemination of scientific research documents, whether they are published or not. The documents may come from teaching and research institutions in France or abroad, or from public or private research centers.

L'archive ouverte pluridisciplinaire **HAL**, est destinée au dépôt et à la diffusion de documents scientifiques de niveau recherche, publiés ou non, émanant des établissements d'enseignement et de recherche français ou étrangers, des laboratoires publics ou privés.

34 Few studies are available in the literature to understand the fate of fragrances after their application
35 on the skin surface. The analysis of perfumes is usually performed by gas chromatography (GC) to
36 separate, identify, and quantify the different components. The headspace (HS) technique can be used
37 for sampling perfume molecules released in the gas phase above a solid or liquid layer. Vuilleumier *et*
38 *al.* [2] applied this technique to characterize the diffusion rates of volatile compounds from the skin as
39 a function of the topical matrix. Fragrances were diluted in ethanol or introduced into a soap base.
40 After application on the skin, volatile compounds evaporated in the HS were trapped on a porous poly-
41 diphenyl phenylene oxide resin of Tenax[®]. This study highlights the complexity of evaporation
42 phenomena in relation to the chemistry of volatile molecules and their interactions with skin lipids at
43 the surface. Moreover, it is important to consider the disadvantages of the dynamic technique, such
44 as its lack of responsibility to other surfaces and the requirement of specific equipment for example.
45 Additionally, the article does not provide details on the system setup, specifications, and dimensions.

46 Behan *et al.* [3] also used the same headspace technique to quantify fragrances on the skin. To highlight
47 the physicochemical interactions between skin lipids and volatile molecules, the evaporation profile of
48 a mixture of fragrances from the skin was compared to evaporation from a vitreous ceramic tile. HS
49 concentrations of the different fragrances trapped in Tenax[®] adsorbent were. Results showed
50 significant differences between the two surfaces. The authors concluded that skin is not an inert
51 surface; it interacts with perfume, slows its evaporation, and is time-dependent. Therefore, the HS
52 analysis should be carried out at several stages of evaporation to provide a better overview of release
53 kinetics and interactions with the support. However, the study by Behan *et al.* (1996) does not detail
54 the glass cell used to sample the perfumes in the HS, particularly regarding volumes, exchange surface,
55 sampling monitoring, and temperature control. These experimental parameters are crucial and must
56 be documented because they greatly influence the evaporation of perfumes.

57 Duffy *et al.* (2018), developed a valuable method for passive headspace sampling of skin volatile
58 emissions in human participants using HS-SPME (solid phase microextraction) GC-Mass Spectrometry
59 (MS) [4]. To achieve this, a glass housing was fixed to the skin on the volar forearm using surgical tape
60 to create an enclosed area of skin headspace. SPME extraction profiles were monitored over time (5–
61 30 min). This non-invasive approach has proven efficient in investigating the volatile composition of
62 human odor. Another system developed in the literature to study evaporation *in vitro* is the use of
63 Franz Cells. Franz Cells are designed to study the diffusion rate of actives and ingredients, particularly
64 in terms of permeation, when applied to the skin. Almeida *et al* [5] examined the evaporation of three
65 fragrance molecules: α -pinene, limonene, and linalool, using dynamic headspace analysis. The
66 temperature was kept at 33°C to mimic human skin surface temperature and *ex vivo* pig skin was
67 placed between the donor and receptor compartments. Similarly, Capetti *et al.* [6] monitored the

68 release of bioactive tea tree oil markers into the atmosphere on pig ear skin using modified Franz cells.
69 The systems proved effective at predicting the evaporation of fragrances on *ex vivo* surfaces, but no
70 optimization was carried out for performing *in vivo* measurements on human skin.

71 Many non-biological models have been used to study occurrences on the surface of the skin [3,7–10].
72 These surface models were employed to explore perfume evaporation [3], cosmetic product
73 application [7,8], and the penetration of active substances [9,10]. Among these models, the glass
74 surface prevents penetration and presents chemical inertia. Another commonly studied surface in the
75 literature is Strat-M[®], a synthetic model specially designed to imitate diffusion through human skin.
76 Penetration experiments [9,10] have been carried out on Strat-M[®], but it has never used to investigate
77 evaporation phenomena. To better understand perfume evaporation from the skin and to assess the
78 influence of specific parameters on the release of fragrance molecules, a methodology combining
79 evaporation studies of surfaces *in vitro* and on the skin *in vivo* could be the answer.

80 Some works have studied penetration *in vitro* [5,11, 6], evaporation *in vitro* [5, 6], or *in vivo* [2,4], but
81 very few studies have focused on both approaches using the same device [3]. Moreover, such studies
82 are relevant as they could enable the development of model surfaces that mimic the release and,
83 therefore, the olfactory perception of perfumes on the skin. Ideally, a modular device allowing dual
84 measurements *in vitro* on different surfaces and *in vivo* on the skin, with the potential to control key
85 experimental parameters, would be developed.

86 This current paper aims to establish this measurement device and an analysis method for evaporation
87 studies both *in vitro*, on different types of model surfaces, and *in vivo*, on the skin of volunteers. This
88 device should enable the modulation of several parameters, such as temperatures, headspace
89 volumes, measurement times, and exchange surfaces, simultaneously. The system was developed
90 based on Franz cells used for transdermal diffusion testing. A perfume composed of eight fragrance
91 molecules in ethanol was used to measure evaporation in the HS with SPME and GC-FID analysis.
92 Temperature control, time measurements, system seal integrity, volumes, and SPME optimizations
93 were investigated. Finally, the effectiveness and modularity of the system were demonstrated with
94 evaporation studies carried out on four different surfaces: a chemically inert glass surface, the Strat-
95 M[®] model, a perfume test strip, and the skin.

96 **2. Materials and methods**

97 2.1 Perfume composition and preparation

98 **The** first objective was to choose a mixture of molecules that differed in chemical structure and
99 physical properties to represent the chemical complexity in a perfume-type mixture. A summary table
100 detailing the selection criteria is given in Table 1. All the chosen molecules are soluble in ethanol, the

101 solvent for this mixture, and vary in their hydrophobicity (log P; P is the n-octanol-water partition
102 coefficient), chemistry (ester, alcohol, or terpene), boiling temperature, vapor pressure, and different
103 verified retention indices relative to C9-C30 n-alkanes on the DB5 column (RI).

104 Ethyl butyrate (CAS No. 105-54-4), ethyl heptanoate (CAS No. 106-30-9), and ethyl octanoate (CAS No.
105 106-32-1) were obtained from Sigma Aldrich. Ethyl decanoate (CAS No. 110-38-3) was obtained from
106 Fluka, limonene from across Organics (CAS No. 5989-27-5), hexyl cinnamaldehyde (Jasmonal[®]) (CAS
107 No. 101-86-0), and myrcene (CAS No. 123-35-3) from Prodasynt, citronellol (CAS No. 106-22-9) from
108 DRT and ethanol (CAS No. 64-17-5, purity 96%) from VWR.

109 Table 1: Summary table of the physicochemical properties (RI, logP, boiling point, vapor pressure, solubility, and molecular
110 weight) of the eight molecules composing the perfume mixture, ranked according to their RI

Molecule	RI [12]	logP [13]	Boiling point (°C) [14]	Vapor pressure (mmHg at 25°C) [13]	Molecular weight (g/mol) [13]
Ethyl butyrate	804	1.85	121	14	116.16
Myrcene	992	4.17	167	2.1	136.23
Limonene	1030	4.57	176	1.55	136.24
Ethyl heptanoate	1080	3.33	188	0.68	158.24
Ethyl octanoate	1198	3.84	208	0.020	172.26
Citronellol	1233	3.91	225	0.020	156.27
Ethyl decanoate	1398	4.86	245	0.034	200.32
Hexyl cinnamaldehyde	1754	5.33	308	0.002	216.32

111 Each component was present at 1% (w/w) except citronellol and hexyl cinnamaldehyde, which were
112 at 2% (w/w) in a 96% ethanol solution to best represent an “eau de toilette”, where fragrance
113 ingredients are solubilised in the solvent and account for 10% of the total mixture. The perfume is kept
114 at 4-6 °C between and after each application. The mixture of volatile molecules complies with IFRA51
115 regulations, with concentrations corresponding to the IFRA standard, and in thus *authorized in*
116 *alcoholic perfumery (cat 4 IFRA) for skin application.*

117 2.2 Preliminary validation of the SPME experimental and analytical protocol for perfume 118 evaporation: Semi-quantification of different fragrances

119 Parameters studied at this step include the equilibration time with a fixed trapping time, and then the
120 trapping time with a fixed equilibration time, optimized in the previous step.

121 To achieve this, the optimization was performed in a classical closed 20mL amber glass vial. The
122 mixture of molecules was applied to the bottom of the vial, and the system was sealed with a septum.
123 The SPME technique was then used to extract and concentrate the volatile compounds present in the
124 HS. The stationary phase grafted was a Divinylbenzene/Carboxen/Polydimethylsiloxane
125 (DVB/CAR/PDMS) stationary phase. This coating was chosen for its affinity with volatile and semi-

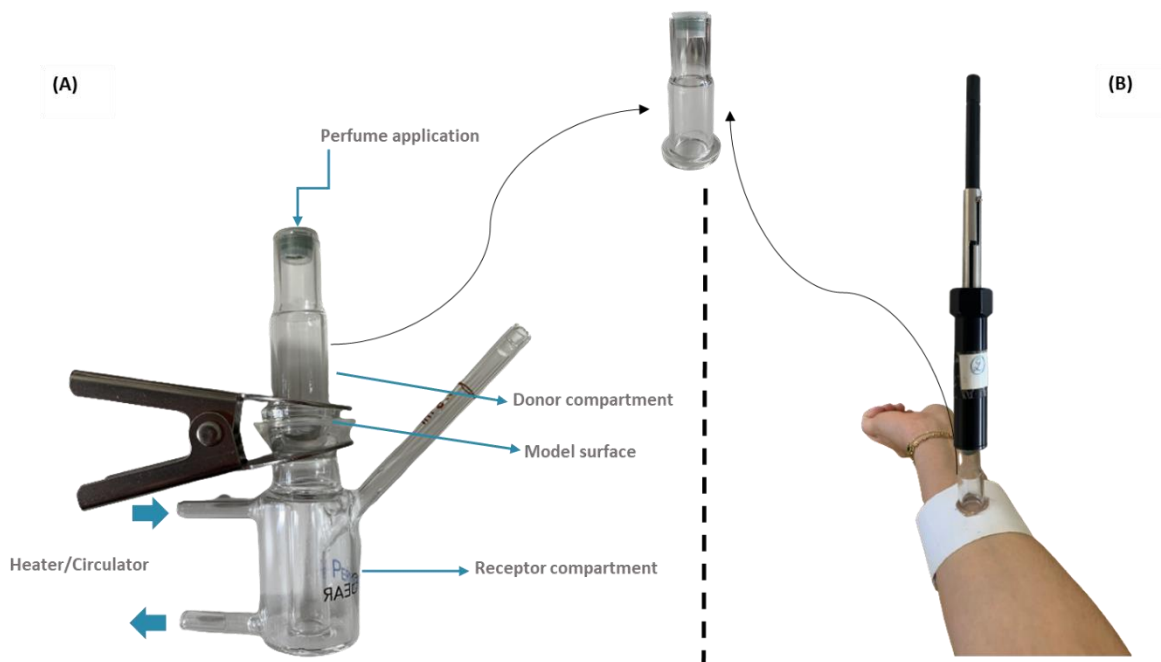
126 volatile compounds from C3 to C20 [15,16], after preliminary tests, not shown here. After the
127 equilibration time, which corresponds to the time given to molecules in the liquid phase to evaporate
128 into the HS, the fiber was positioned in the HS above the solution during a second step, called the
129 trapping time, which corresponds to the equilibrium between the solid phase of the fiber and the
130 gaseous phase.

131 The compounds present after equilibration and trapping times on the fiber were then analysed using
132 an Agilent 8860 GC with a Flame Ionization Detector (FID). They were desorbed in the injector with a
133 split ratio of 1:25, at 260°C for 2 minutes for effective and complete injection. Compounds were
134 separated on an HP-5 column (30 m x 0.32 mm x 0.25µm film thickness) with hydrogen as the carrier
135 gas at a constant flow rate of 1.5 mL/min. The oven temperature program was initially set at 60°C,
136 then raised to 160°C at a rate of 25°C/min, and then increased to 250°C at a rate of 40°C/min. The FID
137 detector was maintained at 250°C, with an airflow rate of 300 mL/min, an H₂ flow rate of 30 mL/min,
138 and an N₂ gas makeup flow rate of 25 mL/min. The components were separated with a resolution
139 greater than 1.5 and identified according to their respective retention indices. The obtained
140 chromatogram will enable the quantification of the compounds released into the headspace above the
141 surface studied. Automatic integration of the peaks is performed by the Agilent software “Agilent
142 OpenLab Control Panel”, which provides the peak areas, enabling the quantification of each compound
143 in the perfume mixture. Note that after each analysis, a fiber injection blank was performed to confirm
144 the absence of residues.

145 2.3 The system adapted for *in vitro* and *in vivo* evaporation studies

146 To study the phenomenon of evaporation on specific surfaces, an innovative system was designed and
147 developed to enable both *in vivo* and *in vitro* measurements, ensuring consistency of analysis and
148 comparison of results. The principle of this setup is depicted in Figure 1 and is based on Franz cells,
149 which are typically used to study penetration but, in the case of the present study, are adapted for
150 evaporation studies. The Franz cell, obtained from Perme Gear.de, is composed of three different
151 parts: the donor compartment (15 mm clear jacketed Franz Cell with a flat ground joint) where the
152 samples are introduced, the receptor compartment (7.5 ml volume) where the diffused components
153 are generally analysed, and the part in-between where the “model” membrane or material is inserted
154 to conduct the permeation study. Interestingly, the temperature of the receptor compartment can be
155 controlled. The adaptation to the purpose of the study consisted of modifying the height, the volume,

156 and the sealness of the donor compartment, which were the first three parameters studied and
157 optimized.



158 Figure 1: Set-ups: (A) *in vitro* using the Franz cell concept with the skin model positioned between the donor compartment
159 and the receptor compartment, and (B) *in vivo*, using the same donor compartment as the Franz cell concept
160 Regarding sealness, based on a literature survey [5], parafilm or a 9 mm diameter Molded
161 Thermogreen® LB-2 Septa GC septum were tested to obtain the best closed-sealed system. The donor
162 compartment height, initially 20 mm, was also optimized and adapted for the total insertion of the
163 SPME fiber and finally set at 50 mm with a final volume of 7 ml.

164 In the in-between zone, the studied perfume mixture was applied to various model surfaces, both *in*
165 *vitro* (Figure 1A) and *in vivo* on the skin (Figure 1B), to test the system's flexibility for different kinds of
166 supports.

167 Surfaces studied were:

168 For *in vitro* tests: i) glass lamellas from Grosseron as a chemically inert surface, ii) a perfume test strip,
169 commonly used in perfumery iii) the Strat-M®, purchased from Merck, a model for permeation tests.

170 For *in vivo* tests: the forearm of a volunteer, cleaned with ethanol before each application.

171 The surface was positioned between the donor compartment and the receiver, thermostated at 32°C.
172 The mixture was applied to the 177 mm² surface, covered by the donor compartment, and the system
173 was sealed at the top of the donor compartment and in the in-between zone with a clamp. The SPME
174 technique was then used with the optimized equilibration and trapping times, enabling the analysis of
175 the quantities evaporated from the studied surface by GC-FID. For the *in vivo* measurements (Figure
176 1B), the system was adapted as follows: the donor compartment was attached to a wristband, whose

177 tightness can be adapted to ensure a tight seal between the donor compartment and the skin. The
178 same procedure was then followed from the application of the mixture to GC analysis, as illustrated
179 with the setups in Figure 1.

180 2.4 Temperature control

181 The last parameter studied during the system optimization is temperature, which indeed impacts the
182 evaporated quantities. Therefore, it must be controlled. To observe the influence of temperature on
183 the evaporation of a specific molecule and compare it with that on the skin, where the average
184 temperature is 32°C, three different temperatures were selected: 27, 32, and 37°C for the receptor
185 compartment.

186 2.5 Data analysis

187 The statistical analyses of collected data were performed using XLSTAT software from Addinsoft
188 (version 2012). All the measurements were carried out in triplicates, and then the average values, the
189 standard deviations and the coefficients of variation (ratio of the standard deviation to the mean) were
190 calculated. An analysis of variance (ANOVA) was applied to the data to determine when the
191 temperature effect was significant ($P \leq 0.05$).

192 **3. Results & Discussion**

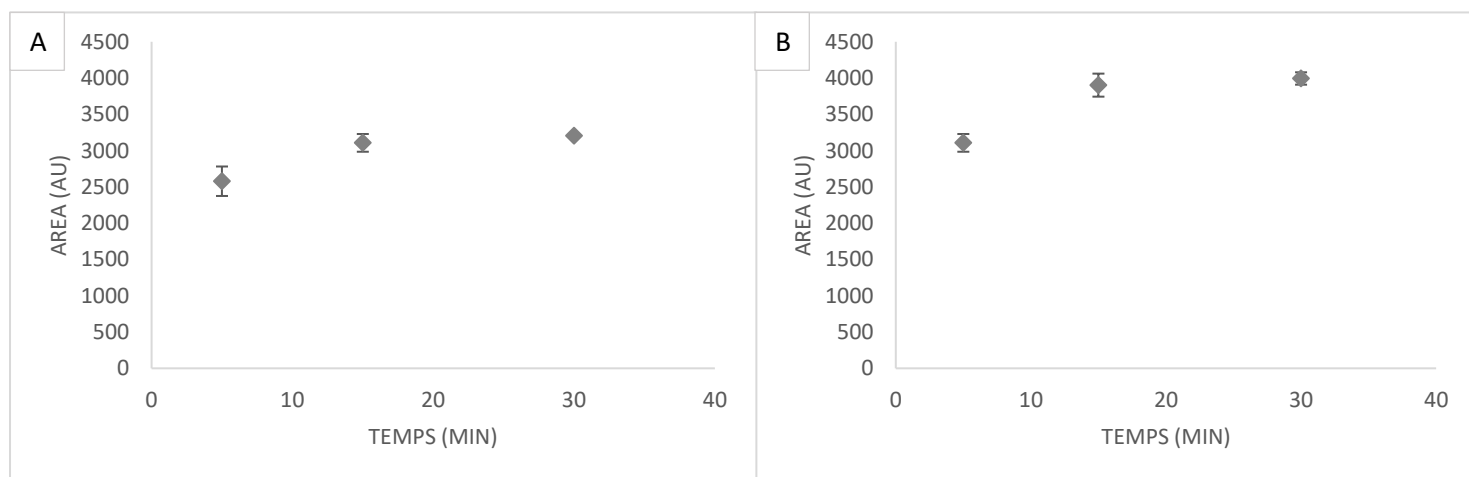
193 **The** objective was to set up a measurement device and an analysis method to monitor the evaporation
194 of fragrance molecules on various surfaces, both *in vitro* on different types of model surfaces and *in*
195 *vivo directly* on the skin of volunteers. This device would allow for the modulation of key parameters
196 such as temperatures, headspace volumes, measurement times, exchange surface, and more. As a first
197 step, SPME parameters were investigated and optimized in glass vials, which serve as a starting point
198 of a simple setup where various optimizations were carried out to achieve efficient results and
199 coherence with the main objective of the system: studying perfumes and fragranced cosmetics. The
200 device was then developed and adapted to glass lamellas, with optimizations made on the system's
201 sealness, volume, and temperature control. Finally, the effectiveness and the modularity of the system
202 were demonstrated through evaporation studies carried out on three other surfaces: a perfume test
203 strip, the Strat-M® model, and the skin surface.

204 3.1 Optimization of equilibration and trapping times using SPME

205 To study and understand the evaporation phenomena occurring after the application of a perfume on
206 a surface, the first parameters investigated were the equilibration and SPME trapping times. The
207 objective was to evaluate the influence of each time phase on the evaporated quantities and then
208 select the most appropriate times that will enable the quantification of the different fragrance
209 molecules. According to the literature [4], three different equilibration times, 5, 15, and 30 minutes,

210 were tested with a constant trapping time of 5 minutes. Then, three different trapping times, 5, 15,
211 and 30 minutes, were tested with a constant equilibration duration of 15 minutes, optimized in the
212 previous step. Alongside the technical aspects that guided the choices for this study, the study was
213 also adapted for *in vivo* use on assessors. The measurement times had to maintain a balance between
214 performance and feasibility. Indeed, for *in vivo* studies, it is challenging to exceed 30 minutes.

215 Results are shown in Figure 2 for ethyl heptanoate, an intermediate compound concerning volatility.
216 Areas increase between 5 and 15 minutes and then remain constant until 30 minutes, both for
217 equilibration time (Figure 2A) and trapping time (Figure 2B), demonstrating appropriate conditions
218 allowing for optimized measurement duration and quality in the obtained results. For the other
219 molecules of the perfume, results have shown that the balance is quickly established for the small,
220 volatile molecules but it is more difficult to achieve for the less volatile molecules. A judicious choice
221 must therefore be made to give all types of volatile molecules time to adsorb and/or absorb onto the
222 fiber. According to the literature, it is important to operate very close to equilibrium conditions to
223 ensure reproducibility [17]. The molecules present in a fragrance have a wide range of volatility, which
224 is why a compromise must be made between trapping time and balance to reach the equilibrium of
225 most molecules. In the case of this study, consistent results with good repeatability for all perfume
226 molecules were obtained at equilibration and trapping times set at 15 minutes. These time conditions
227 are similar to those set by Duffy *et al.*[4].



228 **Figure 2:** Areas in triplicate reflecting the quantities evaporated, obtained for ethyl heptanoate by GC-FID when applied on
229 a glass surface A) for three different equilibration times, 5, 15, and 30 minutes, and a constant trapping time of 5 minutes,
230 B) for three different trapping times, 5, 15, and 30 minutes, with a constant equilibration time of 15 minutes

231 3.2 System optimisation

232 The described system, as already mentioned, is based on Franz cells, adapted in the case of this study
233 for evaporation studies. Once the SPME equilibration and trapping times for perfume analysis were
234 chosen, modifications were made to the initial donor compartment concerning its sealness to ensure
235 the repeatability of measurements, as well as its height and volume. The different modifications of this

236 part of the device were carried out with glass lamellas in the in-between zone. The advantage of using
237 glass is that it is a chemically inert surface with no porosity, thus eliminating any permeation
238 phenomena, allowing for the sole consideration of evaporation phenomena.

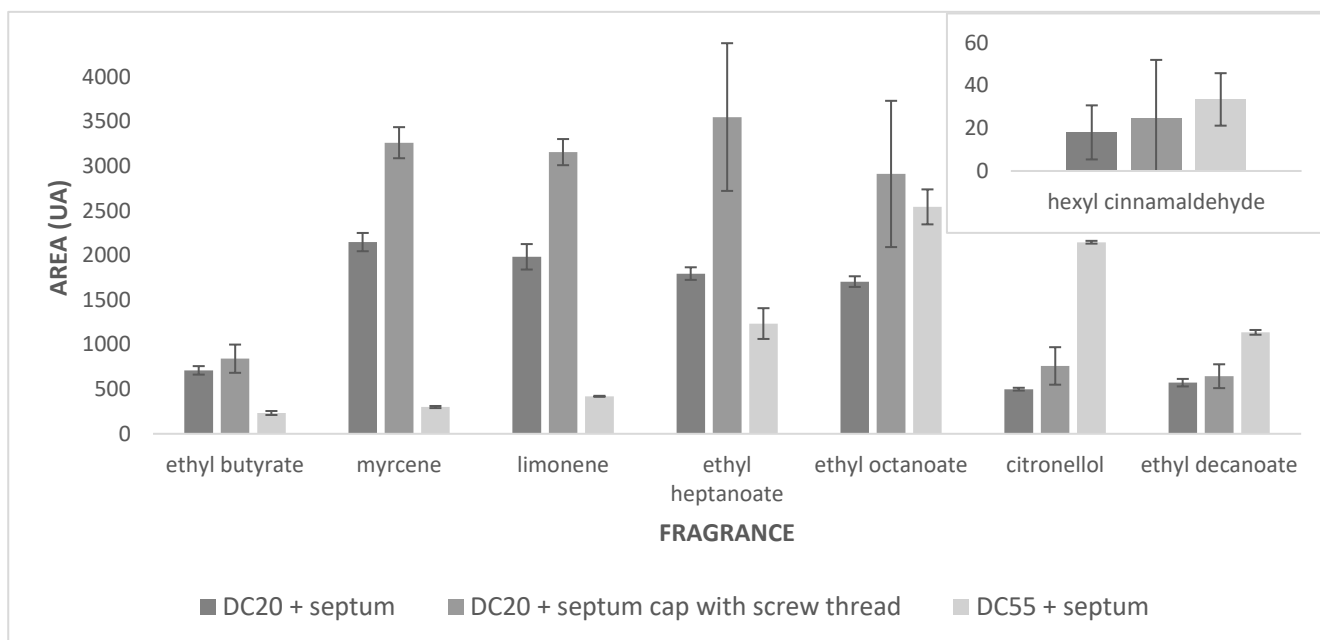
239 3.2.1 Sealness of the device

240 The areas of the eight fragrance compounds are presented in Figure 3. The compounds are sorted in
241 order of retention time. Two sealness conditions were compared: parafilm and a septum aluminum
242 cap. In the initial setup introduced by Almeida *et al* [5], parafilm is positioned at the top of the donor
243 compartment. Parafilm makes the system sealed, which is suitable for penetration studies. However,
244 for evaporation studies and the comparison of fragrance retention on surfaces, parafilm is not ideal.
245 This is because it can potentially retain molecules, leading to interactions between the parafilm and
246 the fragrances. Therefore, the parafilm was replaced with a septum aluminum cap, which is specially
247 designed to avoid interactions with the mixture of fragrances. The peak areas shown in Figure 3
248 indicate higher quantities evaporated with the aluminum cap for all compounds. It should be noted,
249 however, that the results show significant standard deviations, particularly for ethyl heptanoate, ethyl
250 octanoate, and hexyl cinnamaldehyde. As the standard deviations are still not optimal, further
251 improvements to the system are necessary.

252 3.2.2. Height of the donor compartment

253 Considering the feasibility of the system *in vivo*, it was necessary to ensure that the height of the
254 system could be adjusted to maintain reproducibility of measurements. The height must be sufficient
255 to allow for the release of the SPME fiber's full length while also maintaining a 5 mm distance from the
256 skin. Therefore, a higher donor compartment of 55 mm (DC55), replacing the initial 20 mm one (DC20),
257 was set up with the septum cap on top. Results are shown in Figure 3. Areas decreased significantly
258 for most compounds except for the least volatile ones (citronellol, ethyl decanoate, and hexyl
259 cinnamaldehyde). This decrease can be attributed to the increase in the HS volume, which modifies
260 the equilibrium conditions. The increased volume favors the transition to the gaseous phase.
261 Consequently, small molecules may remain in the HS without being adsorbed and/or absorbed onto
262 the fiber, while heavier molecules, which are more concentrated in the HS, can more easily exchange
263 with the stationary phase of the fiber. Additionally, a reduction in standard deviations was observed.
264 In conclusion, the developed device has proven to be sealed, providing repeatable measurements

265 under fixed conditions, allowing for the evaporation of any type of fragrance molecules, whether
266 volatile or less volatile.



267 **Figure 3:** Average area reflecting the quantities evaporated obtained for each compound by GC-FID when the fragrance
268 mixture is applied on a glass surface for three different systems with their respective standard deviations, ranked according
269 to their RI

270 3.2.3. Temperature control

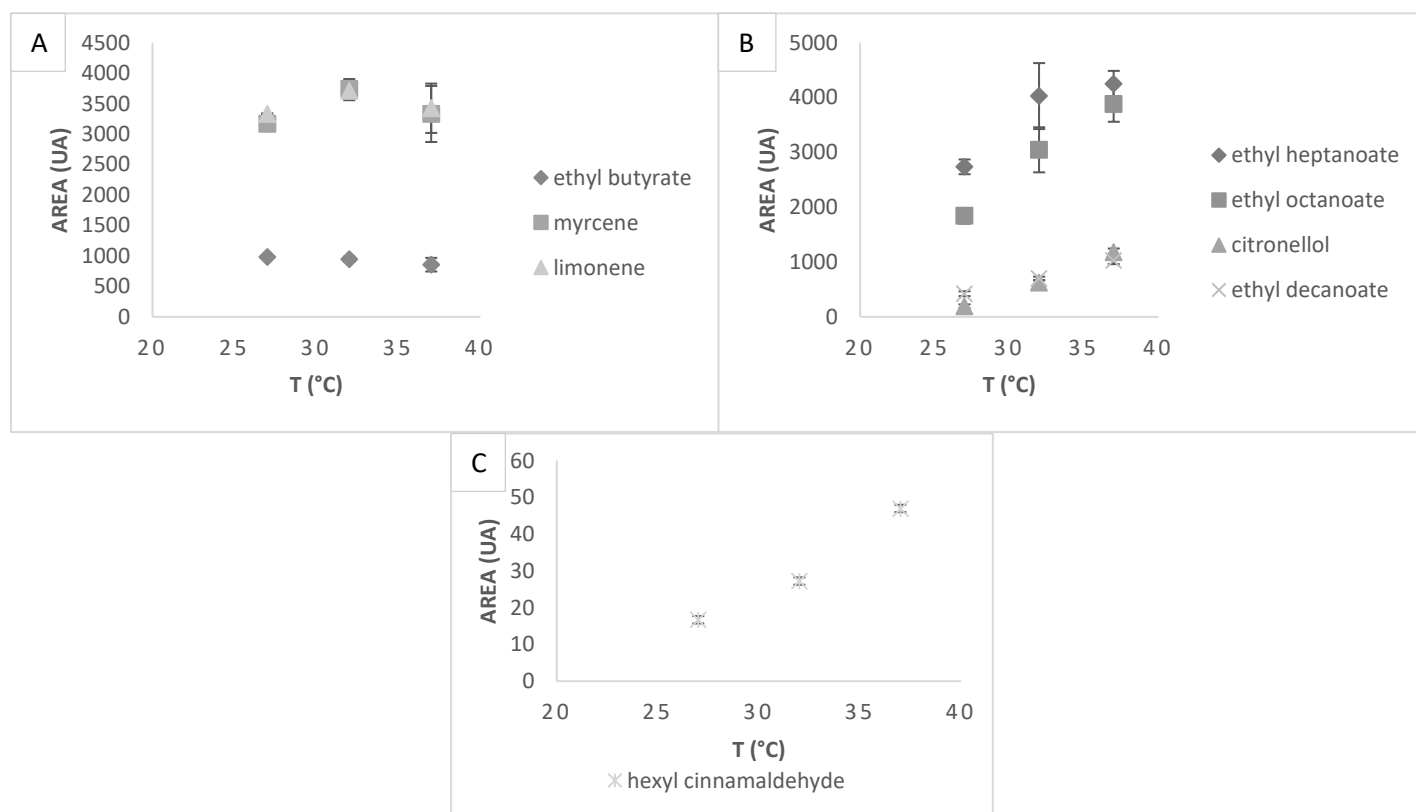
271 Experimental observations on 10 volunteers revealed that skin surface temperature can vary, even
272 within the same zone, with temperatures ranging from 27.5 to 31.9. Additionally, a notable difference
273 in skin surface temperature can be observed depending on the area of the body [18]. Given that
274 fragrances can be applied to different parts of the body, temperature variation can significantly impact
275 the evaporation phenomenon and must be considered. To highlight the influence of skin temperature
276 on molecule evaporation, three biological temperatures were selected: 27, 32, and 37 °C for the
277 receptor compartment.

278 The results presented in Figure 4 highlight the effect of temperature on the evaporated quantities of
279 the different fragrances. Two different behaviors were observed according to ANOVA statistical tests
280 ($P \leq 0,05$): firstly, for some compounds, no significant effect was observed with increasing temperature
281 (Figure 4A), whereas a significant increase with temperature was noticed for others (Figures 4B and C).
282 At a constant temperature, when equilibrium is reached, a partition is established between the solid
283 phase of the SPME fiber and the gaseous phase on one hand, and between the residual liquid phase
284 of the fragrance mixture and the gaseous phase on the other hand. Increasing temperature disturbs
285 this thermodynamic equilibrium and shifts the balance towards the air. This is observed
286 experimentally: for the most volatile compounds such as ethyl butyrate, myrcene, and limonene, the
287 evaporated quantities remain constant since their equilibrium hardly depends on temperature.

288 Conversely, for less volatile molecules like ethyl heptanoate, ethyl octanoate, citronellol, ethyl
289 decanoate, and hexyl cinnamaldehyde, their evaporation is more temperature dependent. Therefore,
290 an increase in evaporated quantities is observed experimentally for the least volatile fragrances as the
291 temperature rises.

292 In conclusion, skin temperature variations can indeed impact fragrance release into the headspace.
293 Thus, for *in vitro* and especially *in vivo* measurements, controlling the temperature parameter during
294 evaporation studies is essential. In **the *in vitro* system**, temperature is controlled with water circulation
295 in the receptor compartment, maintaining the temperature of the donor compartment and the studied
296 surface where the mixture is applied constant. To ensure the studied surface is at the desired
297 temperature at the time of measurement, the surfaces are allowed to equilibrate for 15 minutes
298 before fragrance application. For *in vivo* studies, the volunteer is kept at a controlled room
299 temperature, and the skin temperature is measured following a strict protocol.

300 The *in vitro* temperature was set at 32°C to represent a realistic average skin temperature, which can
301 easily vary depending on the area of skin.



302 Figure 4: Average area reflecting the quantities evaporated obtained for the eight compounds by GC-FID. The fragrance
303 mixture was applied on a glass surface for three different system temperatures: 27°C, 32°C, and 37°C

304 3.3 Adaptability of the system to study evaporation *in vitro* and *in vivo*

305 After the development of the device as presented previously, the effectiveness and modularity of the
306 system were investigated on other surfaces, both *in vitro* and *in vivo*. The fragrance release was carried

307 out on three other surfaces: on the Strat-M® model, a perfume test strip, and the forearm of a
308 volunteer. Studying these different surfaces enabled us to demonstrate the effectiveness of the system
309 and gain a better understanding of the evaporation phenomenon.

310 The evaporated quantities obtained for the eight fragrance compounds are shown in Figure 5 for the
311 four scented surfaces. Repeatability was demonstrated for each of the surfaces, proving the
312 modularity of the device both *in vitro* and *in vivo*. The obtained results show the repeatability of the
313 measurements (according to SPME standards) with coefficients of variation ranging from 1 to 17% for
314 all compounds except hexyl cinnamaldehyde, for which coefficients of variation varied between 7 to
315 33%. It is more complicated for this compound as it has difficulty in evaporating, resulting in smaller
316 chromatographic areas and greater fluctuation from one measurement to another, leading to slightly
317 less accurate results.

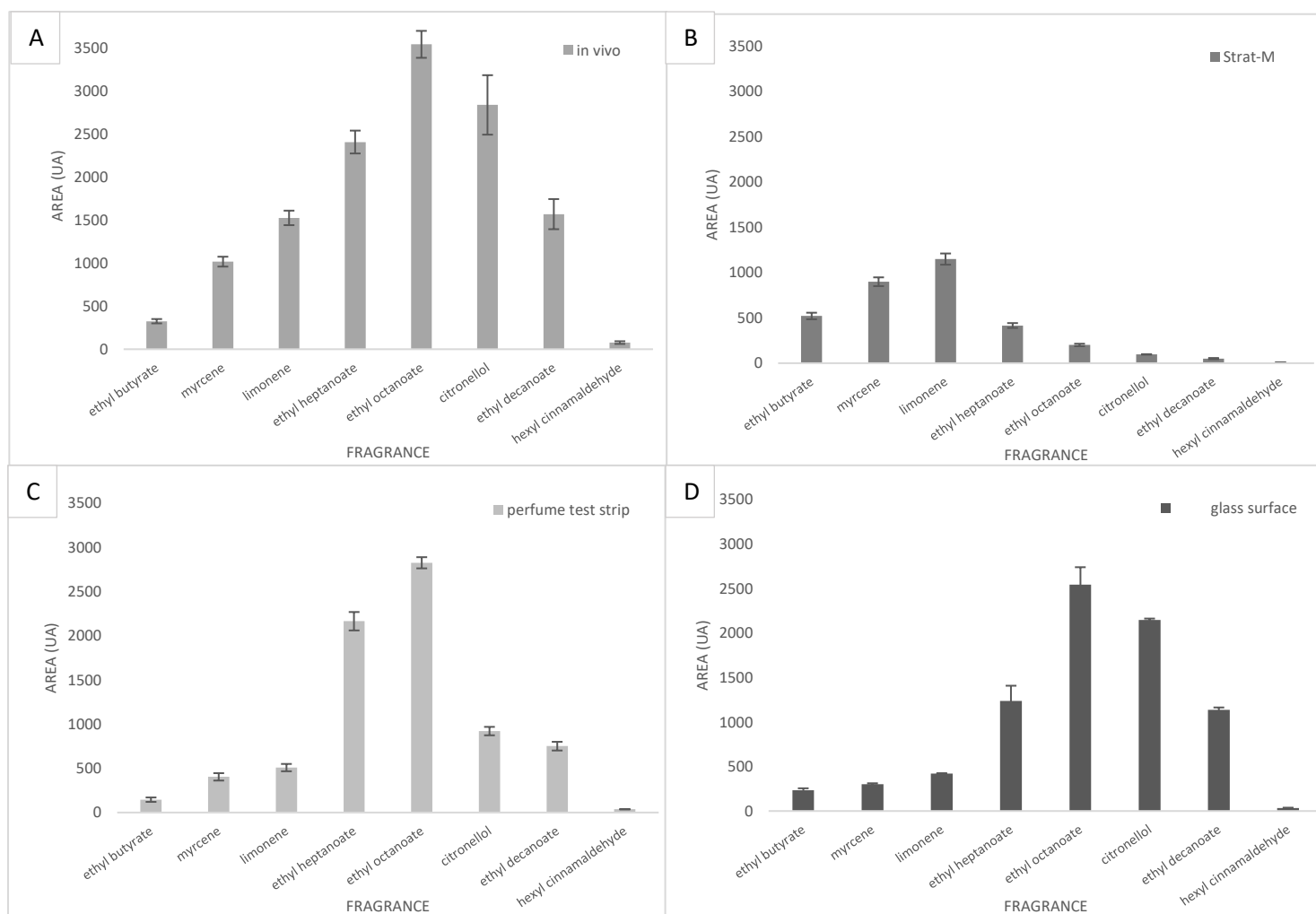
318 The skin is known to have a specific surface physicochemistry due to its structure and composition
319 [19]. Therefore, it was important to prove that the adjustments made to the system on glass were also
320 effective on this complex biological surface. Consequently, the last part of results will be presented as
321 follows: the results obtained and validated on the skin and complementary surfaces.

322 Figure 5A shows the release profile of the model perfume from the skin, with mean areas varying
323 according to the volatility of the compounds and their affinity with the skin. Surface properties of the
324 skin play an important role and influence skin interactions with different fragrance molecules. For
325 example, lipids on the skin will accentuate interactions with more hydrophobic compounds with a
326 higher logP [3]. This is probably the case of the hexyl cinnamaldehyde with a logP of 5.33 (Table 1). The
327 presence of certain lipids on the skin, such as free fatty acids (FFA), makes the skin surface a monopolar
328 basic surface [20]. Indeed, FFA exhibits carbonyl groups which can form hydrogen bonding and are
329 enriched in electrons, thus increasing interactions with water and enhancing a surface monopolar basic
330 behavior [21]. This means that some lipids of the skin could also interact with polar compounds.
331 However, it is important to note that the release phenomena of fragrances on the skin is complex, and
332 other factors such as intrinsic volatility of the molecules, potential absorption in the *stratum corneum*
333 (SC), skin roughness and porosity, and water retention, also play a role in the kinetics of fragrance
334 molecule evaporation.

335 Similar analyses were conducted on three non-biological surfaces: Strat-M® model (Figure 5B),
336 perfume test strip (Figure 5C), and glass (Figure 5D), as discussed previously. Obtained areas varied
337 according to the surface. For instance, the Strat-M®, a multilayer surface composed of
338 polyethersulfone, polyolefin, and a lipid layer, exhibits similar areas for ethyl butyrate, myrcene, and
339 limonene but much lower areas for the other compounds compared to *in vivo* measurements. Such

340 variations in the release profile of a perfume may have a strong influence on its olfactory perception
341 both in intensity and quality. Although the Strat-M is a good candidate for imitating skin diffusion, does
342 not exactly mimic the highly organized intercellular structure of the SC. Indeed, with a relatively thin
343 SC layer, it provides a low-tortuosity pathway which is probably the reason for higher permeability and
344 therefore less retention on the membrane [10]. Even though the Strat-M® has proven to be a good
345 candidate for particular studies on the skin [9,10], it still does not exactly mimic the
346 evaporation/absorption distribution that occurs on the skin after applying a perfumed cosmetic
347 product. Likewise, the perfume test strip, widely used in the perfume industry, made mainly of
348 cellulose, exhibited an evaporation behavior closer to that on the skin due to its hydrophilic and
349 hydrophobic characteristics. Finally, the glass surface, chosen for its chemical inertia, after application
350 of the perfume, spreading of the mixture is observed on the glass substrate, which proves that
351 interactions do take place between the surface and the mixture of compounds. Despite being a
352 completely different surface compared to the other surfaces studied, exhibited a similar evaporation
353 trend to that of the skin.

354 While some interpretations have been provided for initial understanding of the results, the core of this
355 article is to highlight an original innovation in terms of effectiveness, repeatability of measurements,
356 and modularity *in vivo* and *in vitro* by adapting to any type of surface. These results underscore the
357 device's capability to differentiate perfume evaporation on different surface types.



358 **Figure 5:** Average area reflecting the quantities evaporated, obtained for each compound by GC-FID, when the fragrance
 359 mixture was applied on the skin (A), on the Strat-M® surface (B), on a perfume test strip (C), and on a chemically inert glass
 360 surface (D) ranked according to their RI

361 **4. Conclusion**

362 This paper presents a methodological development of a novel device that makes it possible to measure
 363 perfume release in the air above a surface. This device has proven its originality, effectiveness, and
 364 repeatability both *in vitro* on different types of model surfaces and *in vivo* directly on the skin of
 365 volunteers' forearms. A model fragrance composed of eight compounds in ethanol was studied using
 366 HS analyses with SPME GC-FID. **This study has** shown the influence of equilibration and trapping times
 367 on the evaporated quantities, which helped us select the most appropriate conditions for semi-
 368 quantification of different fragrances. With targeted measurement times and optimizations made on
 369 the system's seal, height, volume, and temperature control, the measurement device and the
 370 analytical method were subsequently set up. The modularity of the system was then demonstrated
 371 with evaporation studies carried out on four different surfaces: a chemically inert glass surface, the

372 Strat-M® model, a perfume test strip, and the skin. Further studies can be conducted to evaluate the
373 system's modularity on surfaces such as textiles [22,23] or even *ex vivo* skin.

374 The results obtained from this study underscore the fact that retention of fragrance molecules *in vivo*
375 varies according to their affinity with the skin, their potential interactions, and their intrinsic volatility.
376 The device developed in this study can provide a better understanding of the evaporation phenomena
377 of fragrance molecules and its link with the physico-chemical properties of the skin. The study of
378 fragrance release on *in vitro* model surfaces would offer a solution for standardized fragrance
379 evaluation and a better understanding of retention on the skin. This approach eliminates skin inter-
380 individual variability and facilitates the evaluation of the influence of specific parameters on the
381 retention of fragrances. It will also be capable of determining which materials exhibit skin-like behavior
382 in terms of evaporation phenomena. The next step will be to go even further than fragrance molecules
383 in ethanol but also investigate in greater depth fragrance and active ingredients release in more
384 complex cosmetic products after application on the skin.

385 References:

- 386 (1) Carles, J. Method of Creation & Perfumery. *Soap, Perfumery & Cosmetics* **1961**.
- 387 (2) Vuilleumier, C.; Flament, I.; Sauvegrain, P. Headspace Analysis Study of Evaporation Rate of
388 Perfume Ingredients Applied onto Skin. **1995**, *17* (61–76).
- 389 (3) Behan, J. M.; Macmaster, A. P.; Perring, K. D.; Tuck, K. M. Insight into How Skin Changes
390 Perfume. *Int J Cosmet Sci* **1996**, *18* (5), 237–246. [https://doi.org/10.1111/j.1467-](https://doi.org/10.1111/j.1467-2494.1996.tb00154.x)
391 [2494.1996.tb00154.x](https://doi.org/10.1111/j.1467-2494.1996.tb00154.x).
- 392 (4) Duffy, E.; Albero, G.; Morrin, A. Headspace Solid-Phase Microextraction Gas Chromatography-
393 Mass Spectrometry Analysis of Scent Profiles from Human Skin. *Cosmetics* **2018**, *5* (4), 62.
394 <https://doi.org/10.3390/cosmetics5040062>.
- 395 (5) Almeida, R. N.; Costa, P.; Pereira, J.; Cassel, E.; Rodrigues, A. E. Evaporation and Permeation of
396 Fragrance Applied to the Skin. *Ind. Eng. Chem. Res.* **2019**, *58* (22), 9644–9650.
397 <https://doi.org/10.1021/acs.iecr.9b01004>.
- 398 (6) Capetti, F.; Sgorbini, B.; Cagliero, C.; Argenziano, M.; Cavalli, R.; Milano, L.; Bicchi, C.; Rubiolo, P.
399 Melaleuca Alternifolia Essential Oil: Evaluation of Skin Permeation and Distribution from Topical
400 Formulations with a Solvent-Free Analytical Method. *Planta Med* **2020**, *86* (06), 442–450.
401 <https://doi.org/10.1055/a-1115-4848>.
- 402 (7) Eudier, F.; Grisel, M.; Savary, G.; Picard, C. Design of a Lipid-Coated Polymeric Material Mimic
403 Human Skin Surface Properties: A Performing Tool to Evaluate Skin Interaction with Topical
404 Products. *Langmuir* **2020**, *36* (17), 4582–4591. <https://doi.org/10.1021/acs.langmuir.0c00133>.
- 405 (8) Bhushan, B.; Tang, W. Surface, Tribological, and Mechanical Characterization of Synthetic Skins
406 for Tribological Applications in Cosmetic Science. *J. Appl. Polym. Sci.* **2011**, *120* (5), 2881–2890.
407 <https://doi.org/10.1002/app.33340>.
- 408 (9) Haq, A.; Goodyear, B.; Ameen, D.; Joshi, V.; Michniak-Kohn, B. Strat-M® Synthetic Membrane:
409 Permeability Comparison to Human Cadaver Skin. *International Journal of Pharmaceutics* **2018**,
410 *547* (1–2), 432–437. <https://doi.org/10.1016/j.ijpharm.2018.06.012>.
- 411 (10) Arce, F. J.; Asano, N.; See, G. L.; Itakura, S.; Todo, H.; Sugibayashi, K. Usefulness of Artificial
412 Membrane, Strat-M®, in the Assessment of Drug Permeation from Complex Vehicles in Finite
413 Dose Conditions. *Pharmaceutics* **2020**, *12* (2), 173.
414 <https://doi.org/10.3390/pharmaceutics12020173>.
- 415 (11) Ng, S.-F.; Rouse, J. J.; Sanderson, F. D.; Meidan, V.; Eccleston, G. M. Validation of a Static Franz
416 Diffusion Cell System for In Vitro Permeation Studies. *AAPS PharmSciTech* **2010**, *11* (3), 1432–
417 1441. <https://doi.org/10.1208/s12249-010-9522-9>.
- 418 (12) *Flavornet*. Flavornet and Human odor space. <https://www.flavornet.org/flavornet.html>
419 (accessed 2023-06-12).
- 420 (13) PubChem. *PubChem*. <https://pubchem.ncbi.nlm.nih.gov/> (accessed 2023-06-12).
- 421 (14) *Santé et sécurité au travail*. INRS. <https://www.inrs.fr/> (accessed 2023-06-12).
- 422 (15) Papet, Y.; Brunet, B.; Mura, P. *Headspace* (HS) et micro-extraction en phase solide (SPME).
423 Théorie et applications. *Ann Toxicol Anal* **2010**, *22* (2), 75–79.
424 <https://doi.org/10.1051/ata/2010022>.
- 425 (16) Douny, C.; Dufourny, S.; Brose, F.; Verachtert, P.; Rondia, P.; Lebrun, S.; Marzorati, M.; Everaert,
426 N.; Delcenserie, V.; Scippo, M.-L. Development of an Analytical Method to Detect Short-Chain
427 Fatty Acids by SPME-GC–MS in Samples Coming from an in Vitro Gastrointestinal Model. *Journal*
428 *of Chromatography B* **2019**, *1124*, 188–196. <https://doi.org/10.1016/j.jchromb.2019.06.013>.
- 429 (17) MERCK. SPME for GC Analysis. **2020**, No. MK_BR1410EN.
- 430 (18) Benedict, F. G.; Miles, W. R.; Johnson, A. The Temperature of the Human Skin. *Proc Natl Acad Sci*
431 *U S A* **1919**, *5* (6), 218–222.
- 432 (19) Eudier, F.; Savary, G.; Grisel, M.; Picard, C. Skin Surface Physico-Chemistry: Characteristics,
433 Methods of Measurement, Influencing Factors and Future Developments. *Advances in Colloid*
434 *and Interface Science* **2019**, *264*, 11–27. <https://doi.org/10.1016/j.cis.2018.12.002>.

- 435 (20) Mavon, A.; Zahouani, H.; Redoules, D.; Agache, P.; Gall, Y.; Humbert, Ph. Sebum and Stratum
436 Corneum Lipids Increase Human Skin Surface Free Energy as Determined from Contact Angle
437 Measurements: A Study on Two Anatomical Sites. *Colloids and Surfaces B: Biointerfaces* **1997**, *8*
438 (3), 147–155. [https://doi.org/10.1016/S0927-7765\(96\)01317-3](https://doi.org/10.1016/S0927-7765(96)01317-3).
- 439 (21) Lampe, M. A.; Burlingame, A. L.; Whitney, J.; Williams, M. L.; Brown, B. E.; Roitman, E.; Elias, P.
440 M. Human Stratum Corneum Lipids: Characterization and Regional Variations. *Journal of Lipid*
441 *Research* **1983**, *24* (2), 120–130. [https://doi.org/10.1016/S0022-2275\(20\)38005-6](https://doi.org/10.1016/S0022-2275(20)38005-6).
- 442 (22) Du, L.; Wang, F.-X.; Yang, J.-L.; Shen, Z.-Y.; Zhao, W.-G.; Zou, F.-Y.; Zhu, H.-F.; Xu, S.-H. Effect of
443 Fabric Parameters on Fragrance Retention. *industria textila* **2020**, *71* (6), 7.
- 444 (23) Hsieh, Y.-L. Liquid Transport in Fabric Structures. *Textile Research Journal* **1995**, *65* (5), 299–307.
445 <https://doi.org/10.1177/004051759506500508>.
446